Published OnlineFirst June 1, 2012; DOI: 10.1158/0008-5472.CAN-11-4062

Cancer Research

Inhibitory Roles of Signal Transducer and Activator of Transcription 3 in Antitumor Immunity during Carcinogen-Induced Lung Tumorigenesis

Shoichi Ihara[1], Hiroshi Kida[1], Hisashi Arase[2], Lokesh P. Tripathi[5,6], Yi-An Chen[4,5,6], Tetsuya Kimura[1,3], Mitsuhiro Yoshida[1], Yozo Kashiwa[1], Haruhiko Hirata[1], Reiko Fukamizu[1], Ruriko Inoue[1], Kana Hasegawa[1], Sho Goya[1], Ryo Takahashi[1], Toshiyuki Minami[1], Kazuyuki Tsujino[1], Mayumi Suzuki[1], Satoshi Kohmo[1], Koji Inoue[1], Izumi Nagatomo[1], Yoshito Takeda[1], Takashi Kijima[1], Kenji Mizuguchi[4,5,6], Isao Tachibana[1], and Atsushi Kumanogoh[1,3]

Abstract

Stat3 mediates a complex spectrum of cellular responses, including inflammation, cell proliferation, and apoptosis. Although evidence exists in support of a positive role for Stat3 in cancer, its role has remained somewhat controversial because of insufficient study of how its genetic deletion may affect carcinogenesis in various tissues. In this study, we show using epithelium-specific knockout mice ($Stat3^{\Delta/\Delta}$) that Stat3 blunts rather than supports antitumor immunity in carcinogen-induced lung tumorigenesis. Although $Stat3^{\Delta/\Delta}$ mice did not show any lung defects in terms of proliferation, apoptosis, or angiogenesis, they exhibited reduced urethane-induced tumorigenesis and increased antitumor inflammation and natural killer (NK) cell immunity. Comparative microarray analysis revealed an increase in $Stat3^{\Delta/\Delta}$ tumors in proinflammatory chemokine production and a decrease in MHC class I antigen expression associated with NK cell recognition. Consistent with these findings, human non–small cell lung cancer (NSCLC) cells in which Stat3 was silenced displayed an enhancement of proinflammatory chemokine production, reduced expression of MHC class I antigen, and increased susceptibility to NK cell–mediated cytotoxicity. In addition, supernatants from Stat3-silenced NSCLC cells promoted monocyte migration. Collectively, our findings argue that Stat3 exerts an inhibitory effect on antitumor NK cell immunity in the setting of carcinogen-induced tumorigenesis. *Cancer Res; 72(12); 1–10. ©2012 AACR.*

Introduction

The importance of inflammatory mediators and cells in the tumor microenvironment has recently become the focus of much attention. In some types of cancer, inflammatory conditions initiate or promote oncogenic transformation, whereas in other types of cancer, genetic and epigenetic changes in malignant cells conversely generate an inflammatory microenvironment that further supports tumor progression (1). In addition, cumulative experimental findings indicate that the immune system controls tumor incidence and growth (2). For instance, in colon and ovarian cancers, the presence of infiltrating CTLs or natural killer (NK) cells is associated with a better prognosis (3, 4). In addition, innate immune cells, such as macrophages, NK cells and dendritic cells, can destroy tumor cells when appropriately activated. T cells from the adaptive arm of the immune system can also attack tumors when activated in a type 1 helper T (Th1) immunologic milieu (5, 6). By contrast, tumor-associated macrophages have been shown to promote cancers, partly through their ability to secrete angiogenic, metastatic, and growth factors (1). Another related myeloid lineage, myeloid-derived suppressor cells, which are increased in cancers, not only suppress antitumor immunity but also directly contribute to tumor growth (7). Therefore, it remains controversial how inflammation and immunity influence tumorigenesis.

Stat3 mediates signals for interleukin-6 (IL-6), IL-11, oncostatin M, leukemia inhibitory factor, and ciliary neurotropic factor, and activates the transcription of various target genes. Although Stat3 was originally identified as an inducible DNA-binding protein that binds an *IL-6–responsive element* within the promoter of hepatic acute phase protein genes, Stat3 is expressed in a variety of cells and tissues and exerts pleiotropic

Authors' Affiliations: [1]Department of Respiratory Medicine, Allergy and Rheumatic Diseases, Osaka University Graduate School of Medicine; [2]Laboratory of Immunochemistry, [3]Department of Immunopathology, World Premier International Research Center (WPI), Immunology Frontier Research Center, and Department of Immunochemistry, Research Institute for Microbial Disease, Osaka University; [4]Graduate School of Frontier Biosciences, Osaka University; [5]National Institute of Biomedical Innovation, Osaka; and [6]Core Research for Evolutional Science and Technology, Japan Science and Technology Agency, Honcho Kawaguchi, Saitama, Japan

Note: Supplementary data for this article are available at Cancer Research Online (http://cancerres.aacrjournals.org/).

Corresponding Author: Hiroshi Kida, Department of Respiratory Medicine, Allergy and Rheumatic Diseases, Osaka University Graduate School of Medicine, 2-2 Yamadaoka, Suita, Osaka 565-0871, Japan. Phone: 81-66879-3833; Fax: 81-66879-3839; E-mail: hiroshi.kida@imed3.med.osaka-u.ac.jp

doi: 10.1158/0008-5472.CAN-11-4062

Published OnlineFirst June 1, 2012; DOI: 10.1158/0008-5472.CAN-11-4062

functions. Because a Stat3 deletion leads to embryonic lethality in mice (8), the physiologic and pathologic significance of Stat3 in adult organs has been investigated using conditional knockout animals generated using the Cre/loxP recombination system (9). These studies revealed that Stat3 exerts a variety of biologic functions, including cell growth, antiapoptosis, and cell motility, depending on the cell types and stimuli. With regard to the role of Stat3 in promoting or inhibiting cancer, Stat3 has been implicated in the survival and proliferation of various cancer cells by upregulating the expression of various genes, including Bcl-xL (10), Mcl-1 (11), cyclin D1 (12), and c-Myc (13). In addition to these cell autonomous effects, Stat3 has been shown to have cancer-promoting properties through "bystander" effects, such as stimulating angiogenesis and regulating inflammatory and immune responses in tumor microenvironments (14). On the basis of these *in vitro* studies with cancer cell lines, *in vivo* tumorigenesis models using tissue-specific knockout mice have revealed that Stat3 promotes tumorigenesis in the colon (15, 16), stomach (17), and pancreas (18, 19) by enhancing tumor-associated inflammation and tumor proliferation. In fact, the association between inflammation and tumorigenesis is very strong in these organs. However, no firm causal relationships with inflammation or infection have been established for lung tumorigenesis (20–22). In addition, the role of Stat3 in carcinogen-induced lung tumorigenesis has not been examined.

In this study, we used urethane-induced lung tumorigenesis models and found that tumorigenesis was significantly reduced in $Stat3^{\Delta/\Delta}$ mice, although these mutant mice did not show any abnormalities in proliferation, apoptosis, or angiogenesis. Interestingly, tumor-associated antitumor inflammation increased in $Stat3^{\Delta/\Delta}$ mice, suggesting that Stat3 signaling is important in evading antitumor immunity during lung tumorigenesis. Of note, microarray analysis identified 2 significant Stat3-mediated pathways. One pathway involves the upregulation of proinflammatory chemokine production by tumor cells in $Stat3^{\Delta/\Delta}$ mice. The other pathway leads to the suppression of NK cell–related MHC class I expression in tumor cells in $Stat3^{\Delta/\Delta}$ mice, which may allow the tumor cells to stimulate NK cell–mediated immunosurveillance. Collectively, our studies with a carcinogen-induced tumorigenesis model revealed a novel role for Stat3 in inhibiting antitumor immunity during lung tumorigenesis.

Materials and Methods

Animal experiments

$Stat3^{\Delta/\Delta}$ mice were generated as previously described (23, 24). Briefly, the *human surfactant protein (hSP)-C* promoter was used to express the reverse tetracycline transactivator (rtTA). In the presence of doxycycline, rtTA binds to the $(tetO)_7$ promoter, activating transcription of the Cre recombinase. *LoxP* sites were inserted into introns 20 and 21 of the *Stat3* gene ($Stat3^{flox}$), in which exon 21 was deleted after recombination to produce the $Stat3^{\Delta}$ locus. Triple transgenic ($Stat3^{\Delta/\Delta}$) and nondeleted littermate ($Stat3^{flox/flox}$) control mice were used for the experiments. Six-week-old mice were intraperitoneally injected with urethane (1 mg/g body weight; Sigma). After 4 to 6 months, the lung tumors were scanned by micro-CT (GE eXplore Locus micro-CT scanner; GE Healthcare). Images were reconstructed and the total lung tumor volume per mouse (TV) was quantified using MicroView analysis software (GE Healthcare). After CT scanning, the mice were sacrificed for each experiment. All protocols were approved by the Institutional Animal Care and Use Committee at Osaka University.

Bronchoalveolar lavage

Mice ($N = 14$ for $Stat3^{flox/flox}$ group and $N = 8$ for $Stat3^{\Delta/\Delta}$ group) were sacrificed with a lethal intraperitoneal phenobarbital injection 6 months after urethane treatment. The trachea was cannulated and the lungs were lavaged 3 times with 1 mL of saline. The volumes of recovered bronchoalveolar lavage (BAL) fluid from mice in both groups were similar. After centrifugation, BAL cells were counted using a hemocytometer to determine total BAL cell count. Differential cell counts based on cell morphology were carried out after cytospin followed by May–Giemsa staining to classify the infiltrating cells as monocytes/macrophages, lymphocytes, neutrophils, or eosinophils. Data were analyzed using JMP version 9.0.2 (SAS Institute). The normality of distribution was examined by visually inspecting Q-Q plots. Two groups ($Stat3^{flox/flox}$ vs. $Stat3^{\Delta/\Delta}$) were compared using the ANOVA model, which included the following factors: the mouse groups, TV, and the interaction between the groups and TV. A 2-sided P value less than or equal to 0.05 was considered significant. A nonparametric analysis was also conducted to confirm the robustness of the ANOVA analysis results.

Immunohistochemistry

Lungs were inflation fixed (25 cmH_2O) with 4% paraformaldehyde/PBS for 1 minute, immersed in the same fixative for 18 hours at 4°C and then processed according to standard methods for paraffin-embedded blocks. Immunohistochemistry (IHC) was carried out on 5-μm thick sections. The following primary antibodies were used: Clara cell secretory protein (CCSP; 1:1,500, rabbit polyclonal; Seven Hills Bioreagents), prosurfactant protein (SP)-C (1:2,000, rabbit polyclonal; Seven Hills Bioreagents), phospho-Stat3 (Tyr705; rabbit polyclonal; Cell Signaling Technology), VEGF receptor (VEGFR)-2 (1:300, rabbit IgG; Cell Signaling Technology), phospho-histone-3 (PH-3; 1:500, rabbit polyclonal; Santa Cruz Biotech), cleaved caspase-3 (1:1,600, rabbit polyclonal; Cell Signaling Technology), and Bcl-xL (1:300, rabbit polyclonal; Cell Signaling).

Cell lines

A549 was obtained from the Japanese Collection of Research Bioresources. KHYG-1 was obtained from Health Science Research Resource Bank. HCC827 and H3255 were kindly gifted from Pasi A. Jänne (Dana-Farber Cancer Institute/Department of Medical Oncology, Boston, MA). HFL-1 was obtained from Riken BioResource Center. NCI-H292, 3T3, H441, and THP-1 were purchased from the American Type Culture Collection.

Western blot analysis and ELISA

Lung tissue was snap-frozen in liquid nitrogen. Frozen tissue was broken into pieces using a mortar and lysed in 5 mL of

Published OnlineFirst June 1, 2012; DOI: 10.1158/0008-5472.CAN-11-4062

T-PER Tissue Protein Extraction Reagent (Pierce). After centrifuging at 1,000 × *g* for 5 minutes, the supernatants were stored at −80°C. Western blot analysis was done using 20 μg of protein and the following primary antibodies: phospho-histone-3 (PH-3; 1:500, rabbit polyclonal; Santa Cruz Biotech), VEGFR-2 (1:250, rabbit IgG; Cell Signaling Technology), phospho-Stat3 (1:1,000, rabbit polyclonal; Cell Signaling Technology), mouse MHC class I (ER-HR52; 1:200, rat monoclonal IgG2a; Santa Cruz), human MHC class I (W6/32; 1:400, mouse monoclonal IgG2a; Santa Cruz), and actin [1:1,000, horseradish peroxidase (HRP)-conjugated goat polyclonal; Santa Cruz]. A goat anti-rabbit IgG (H+L)-HRP conjugated (BioRad) or HRP-goat anti-rat IgG (H+L; Invitrogen) antibody was used as the secondary antibody. The levels of IFN-γ, TNF-α, and IL-6 in the supernatants were determined using quantitative murine sandwich ELISA kits (R&D Systems Inc.) and normalized to the total lung tumor volume.

Microarray analysis

Lung tumors were microdissected and pooled. RNA was extracted with RNAiso Plus (Takara Bio) and purified with an RNeasy Mini Kit (Qiagen). The RNA quality and quantity were analyzed using an Agilent 2100 Bioanalyzer (Agilent Technologies) and NanoDrop ND-1000 (Thermo Fisher Scientific), respectively. Gene expression was analyzed using GeneChips mouse genome 430 2.0 array (Affymetrix) according to the manufacturer's protocol. Arrays were scanned on a GeneChip scanner 3000 (Affymetrix).

Construction of protein–protein interaction networks and functional analysis of the differentially expressed genes by characterization of enriched biologic associations

Protein–protein interactions (PPI) for genes that showed increased or decreased expression in the microarray studies were retrieved from the BioGRID (25) and iRefIndex 8.0 (26) databases using the TargetMine data warehouse (27). Biologic pathway data from KEGG (28) were used to assign functional annotations to the genes in the upregulated and downregulated networks. The overexpression of specific KEGG pathway associations within each network was estimated by carrying out the hypergeometric test within TargetMine. The inferred *P* values were further adjusted for multiple test corrections to control for the false discovery rate using the Benjamini and Hochberg method (29), and the pathway annotations were considered significant if *P* value was less than or equal to 0.05.

Knockdown experiment with siRNA

Cells were transfected with either siRNA against human Stat3 or control cocktail RNAs (B-Bridge International), using Lipofectamine RNAiMAX (Invitrogen) according to the manufacturer's protocol. After a 48-hour incubation, the cells were replated in serum-containing medium (5×10^5/mL) and cultured for another 30 hours. Protein and RNA expression was analyzed by Western blot and TaqMan real-time reverse transcriptase PCR (Applied Biosystems), respectively. The concentrations of CCL5 and CXCL10 in the culture supernatants were determined using quantitative murine sandwich ELISA kit (R&D).

In vitro migration assay

The migration of monocytes (THP-1 cells) was measured by a modified Boyden chamber migration assay. THP-1 cells were loaded into Transwell inserts (5-μm porous membrane; Corning). The culture supernatants of non–small cell lung cancer (NSCLC) cell lines transfected with Stat3 siRNA or control siRNA were placed in the lower chamber. Cells on the upper side of the membrane were removed after 4 hours and the number of migratory cells was determined by Guava ViaCount assays (Millipore).

Cytotoxic assay

Susceptibility to NK cell–mediated cytotoxicity was measured by a conventional 4-hour ^{51}Cr-release assay as previously described (30). Briefly, the target cells, an NSCLC cell line (H3255 and H441) that was transfected with Stat3 or control siRNA, were labeled with ^{51}Cr and mixed with effector cells, KHYG-1 cells, at different effector/target (E/T) ratios. After a 4-hour incubation, the supernatant was collected for liquid scintillation counting. Spontaneous ^{51}Cr-release was measured in target cells incubated without effector cells, and the maximal release was measured by treating the target cells with 5% Triton X-100. The percent specific lysis was determined using the following formula: % specific lysis = 100 × (experimental release − spontaneous release)/(maximum release − spontaneous release).

Statistical analysis

All statistical analyses were done using JMP version 9.0.2 (SAS). Data are expressed as the means ± SE. The differences between the 2 groups were evaluated using 2-sided Student *t* test or ANOVA. *P* values less than 0.05 were considered statistically significant.

Results

Urethane-induced lung tumorigenesis was inhibited in Stat3$^{\Delta/\Delta}$ mice

To investigate the pathologic role of Stat3 in lung tumorigenesis, we first examined urethane-induced tumorigenesis in Stat3$^{\Delta/\Delta}$ mice. Stat3$^{\Delta/\Delta}$ mice did not show any abnormalities in terms of lung size, lung morphology, or respiratory functions before urethane administration (23, 24). At 4 months after urethane injection, we examined the size of the lung tumors by micro-CT (Fig. 1A). Lung tumors had developed in 90.3% (28 of 31) of the Stat3$^{flox/flox}$ mice and 76.9% (10 of 13) of the Stat3$^{\Delta/\Delta}$ mice. The total lung tumor volume per mouse (TV) was significantly decreased in Stat3$^{\Delta/\Delta}$ mice (average 2.9 mm^3 per mouse) compared with Stat3$^{flox/flox}$ mice (average 6.5 mm^3 per mouse; $P = 0.037$; Fig. 1B). A histologic examination revealed that tumors in both mice displayed the same morphologic characteristics of lung adenomatous tumor, except that Stat3$^{\Delta/\Delta}$ mice never acquired large tumors compared with Stat3$^{flox/flox}$ mice (Fig. 1C, Supplementary Fig. S1). IHC for CCSP, a Clara cell marker, and pro-SP-C, an alveolar type II

Published OnlineFirst June 1, 2012; DOI: 10.1158/0008-5472.CAN-11-4062

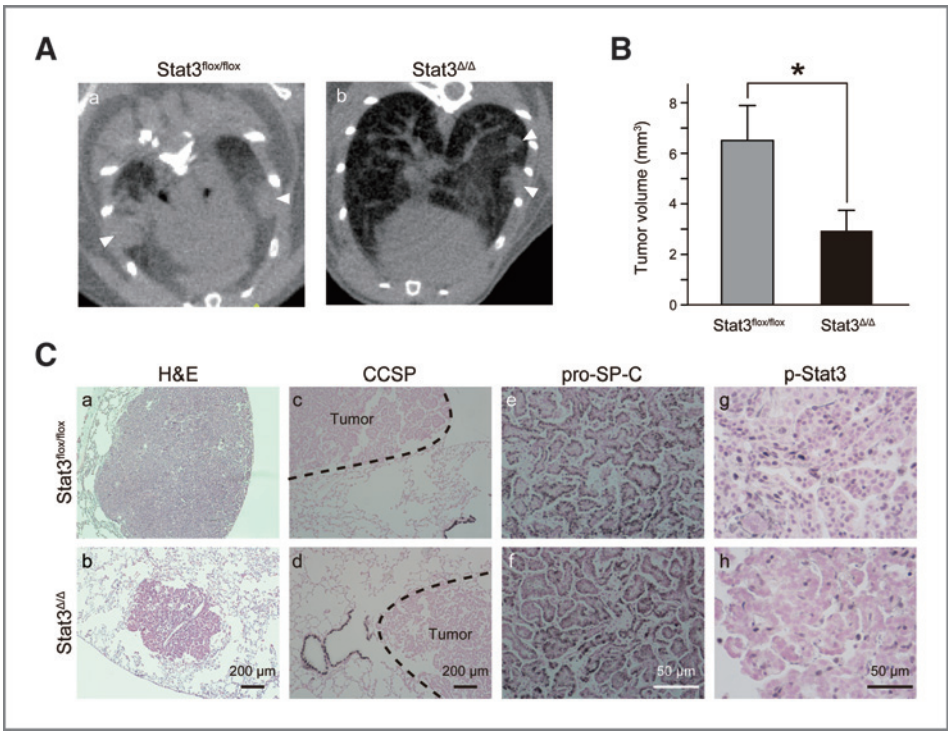

Figure 1. Carcinogen-induced lung tumorigenesis was impaired in $Stat3^{\Delta/\Delta}$ mice. A, representative micro-CT images of $Stat3^{flox/flox}$ (a) and $Stat3^{\Delta/\Delta}$ (b) mice showing lung tumors (arrowheads). Mice were intraperitoneally injected with urethane (1 mg/g body weight) and tumor formation was visualized after 4 months. B, each tumor volume was quantified and the total tumor volume was determined. The total lung tumor volume per each mouse was significantly decreased in $Stat3^{\Delta/\Delta}$ mice. $N = 31$ for $Stat3^{flox/flox}$ group and $N = 13$ for $Stat3^{\Delta/\Delta}$ group. *, $P < 0.05$. C, representative hematoxylin and eosin stain (H&E)-stained sections of tumors in $Stat3^{\Delta/\Delta}$ (b) compared with $Stat3^{flox/flox}$ (a) mice. Immunohistochemical analysis of CCSP (c and d), pro-SP-C (e and f), and phospho-Stat3 (g and h) in lung tumors from $Stat3^{flox/flox}$ (c, e, and g) and $Stat3^{\Delta/\Delta}$ (d, f, and h) mice.

epithelial cell marker, revealed that the tumor cells were CCSP-negative and pro-SP-C–positive, indicating that they developed from alveolar type II epithelial cells (Fig. 1C). IHC for phospho-Stat3 confirmed that the Stat3 expressed in tumor cells was activated in $Stat3^{flox/flox}$ mice but not in $Stat3^{\Delta/\Delta}$ mice, indicating that the tumors in $Stat3^{\Delta/\Delta}$ mice did not originate from progenitor cells that escaped Cre-mediated deletion (Fig. 1C). In addition, we confirmed that the expression and function of Stat3 was intact in myeloid cells and lymphocytes (Supplementary Fig. S2). These findings indicated that a Stat3 deletion in airway epithelial cells inhibited tumor formation in a urethane-induced lung tumorigenesis model.

Proliferation, apoptosis, and angiogenesis in lung tumors in $Stat3^{\Delta/\Delta}$ mice

Previous studies reported that Stat3 is involved in mitosis, survival, and angiogenesis during tumorigenesis. Thus, we examined the possibility that a Stat3 deletion in airway epithelial cells results in impaired mitosis, survival, and angiogenesis in urethane-induced lung tumors. First, we assessed proliferation by IHC and Western blot analysis using phospho-histone-3 (PH-3) as a marker, which was not different between $Stat3^{\Delta/\Delta}$ mice and $Stat3^{flox/flox}$ mice (Fig. 2A and B). Next, we examined apoptosis by immunohistochemically examining cleaved caspase-3. There were few positive cells in both $Stat3^{\Delta/\Delta}$ mice and $Stat3^{flox/flox}$ mice, suggesting that apoptosis plays a minimal role during urethane-induced tumorigenesis (data not shown). In addition, we examined the expression of Bcl-xL, an antiapoptotic protein, by IHC and Western blot analysis and found that there were no apparent differences between $Stat3^{\Delta/\Delta}$ mice and $Stat3^{flox/flox}$ mice (Fig. 2A and B). With regard to vascular development, immunohistochemical analysis for VEGFR-2 showed that the expression of VEGFR-2 was specifically stained in the vascular endothelial cells but not in tumor cells, in which there were no difference between $Stat3^{\Delta/\Delta}$ mice and $Stat3^{flox/flox}$ mice (Fig. 2A). In addition, we did not see significant differences in the levels of VEGFR-2 and VEGF in the lung homogenates between $Stat3^{\Delta/\Delta}$ mice and $Stat3^{flox/flox}$ mice (Fig. 2B and C). These findings unexpectedly showed that Stat3 in tumor cells has a minimal effect on mitosis, apoptosis, and angiogenesis in this model.

Tumor-associated inflammation was augmented in $Stat3^{\Delta/\Delta}$ mice

It is well known that inflammation in the tumor microenvironment acts to either promote or inhibit tumors depending on the tissue type (1). Thus, we next examined the effects of an epithelial cell–specific Stat3 deletion on tumor-associated inflammation in the lung and surprisingly found significantly more inflammatory cells surrounding tumors in $Stat3^{\Delta/\Delta}$ mice compared with $Stat3^{flox/flox}$ mice (Fig. 3A). Therefore, we carried out BAL to count inflammatory leukocytes in the lung. The number of inflammatory cells, including macrophages, lymphocytes, and neutrophils, recovered in the BAL fluid correlated with the TV, suggesting that inflammation correlated with tumor growth. Indeed, the ratios of inflammatory cell numbers to TV were significantly higher in $Stat3^{\Delta/\Delta}$ mice compared with $Stat3^{flox/flox}$ mice (Fig. 3B). The relative concentrations of antitumor inflammatory mediators, such as IFN-γ, TNF-α, and IL-6, to TV were also increased in the lungs of $Stat3^{\Delta/\Delta}$ mice compared with $Stat3^{flox/flox}$ mice (Fig. 3C). Taken together

Published OnlineFirst June 1, 2012; DOI: 10.1158/0008-5472.CAN-11-4062

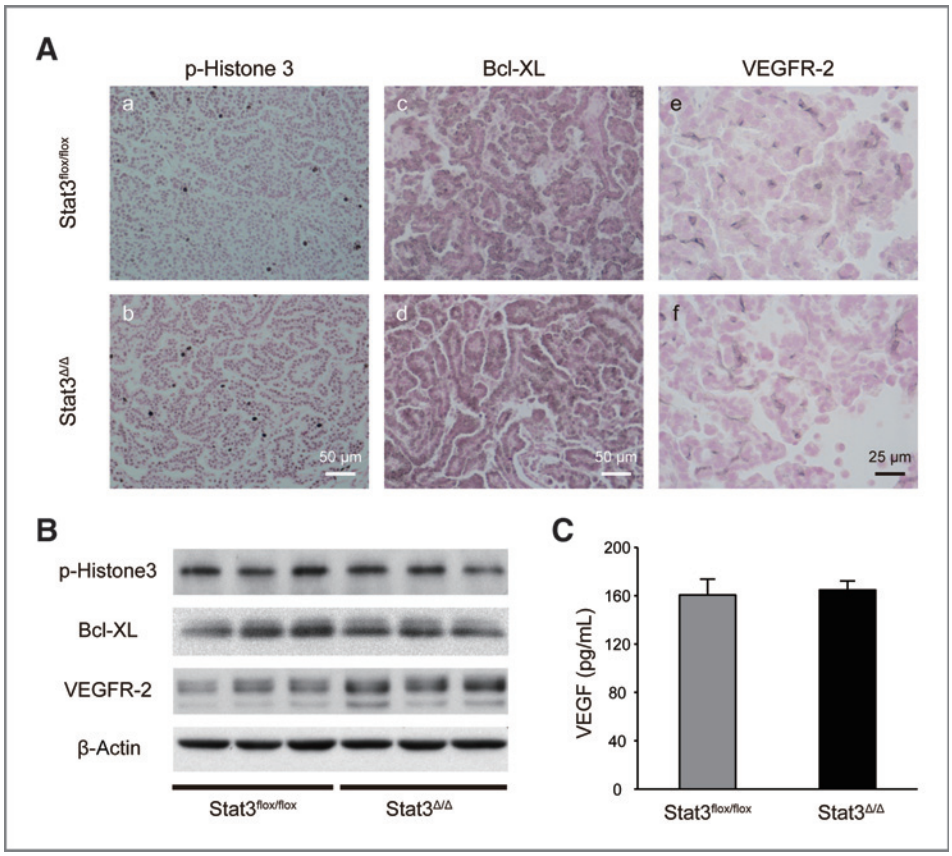

Figure 2. Neither proliferation, apoptosis, nor angiogenesis was impaired in Stat3$^{\Delta/\Delta}$ lung tumors. A, immunohistochemical analysis of phospho-histone-3 (a and b), Bcl-xL (c and d), and VEGFR-2 (e and f) in lung tumors from Stat3$^{flox/flox}$ (a, c, and e) and Stat3$^{\Delta/\Delta}$ (b, d, and f) mice. B, immunoblot analysis of the indicated proteins in the lung homogenates from Stat3$^{flox/flox}$ mice and Stat3$^{\Delta/\Delta}$ mice. $N = 3$ per group. C, ELISA for VEGF in the lung homogenates from Stat3$^{flox/flox}$ mice and Stat3$^{\Delta/\Delta}$ mice. $N = 3$ per group.

with the fact that tumor growth was suppressed in Stat3$^{\Delta/\Delta}$ mice, these data implied that a Stat3 deletion in tumor cells promotes antitumor inflammatory responses in urethane-induced tumorigenesis.

Genome wide mRNA expression profiling revealed the upregulation of proinflammatory chemokines and downregulation of NK-related MHC class I in Stat3$^{\Delta/\Delta}$ mice

To understand the mechanisms underlying the antitumor inflammatory responses evoked in the absence of Stat3 in lung tumor cells, we carried out a microarray analysis using RNA extracted from the tumors. A comparison of gene expression between Stat3$^{\Delta/\Delta}$ and Stat3$^{flox/flox}$ tumors revealed that 298 and 338 genes were upregulated and downregulated, respectively, in Stat3$^{\Delta/\Delta}$ mice compared with Stat3$^{flox/flox}$ mice (Supplementary Tables S1 and S2).

Because most genes function in association with other genes and gene products, to further understand the biologic significance of the different gene expression levels, we retrieved the PPIs for the upregulated and downregulated genes and inferred PPI networks using TargetMine. Next, we investigated the upregulated and downregulated gene expression cum PPI networks (comprising 396 and 490 genes, respectively) for the enrichment of specific KEGG pathway associations (Supplementary Tables S3 and S4). We observed that deleting Stat3 in tumor cells led to a significant increase in genes associated with chemokine production (CCL2, CCL9, CCL12, CCL17, and CCL21c), which were mapped to the enriched KEGG pathway, "chemokine signaling pathway" ($P = 1.53 \times 10^{-4}$) and function in inflammatory immune responses (Fig. 4A). Also, there was a significant decrease in genes involved in NK cell–related MHC class I expression (H2-D1, H2-K1, and H60a), which were mapped to the enriched KEGG pathway, "NK cell–mediated cytotoxicity" ($P = 8.46 \times 10^{-6}$) and are associated with the innate immune system (Fig. 4B). In this context, we hypothesized that a Stat3 deletion promotes chemokine production and inhibits of MHC class I expression in tumor cells, leading to the upregulation of antitumor inflammatory responses.

Stat3 blockade increased chemokine expression in lung epithelial cell lines

To investigate whether Stat3 activation in tumor cells negatively regulates the expression of inflammatory mediators, we suppressed Stat3 expression in NSCLC cells using siRNA transfection. As reported previously, all NSCLC cells showed various degrees of constitutively activated Stat3 (Fig. 5A). Introducing Stat3 siRNA significantly reduced Stat3 expression and upregulated the expression of chemokines, including CCL5 (RANTES) and CXCL10 (IP-10; Fig. 5B and C). To confirm that the inflammatory factors that were produced by Stat3-suppressed NSCLC cell lines affect immunity, we carried out monocyte migration assays using cell culture supernatants from Stat3 siRNA- or control siRNA-transfected cells. As shown

Published OnlineFirst June 1, 2012; DOI: 10.1158/0008-5472.CAN-11-4062

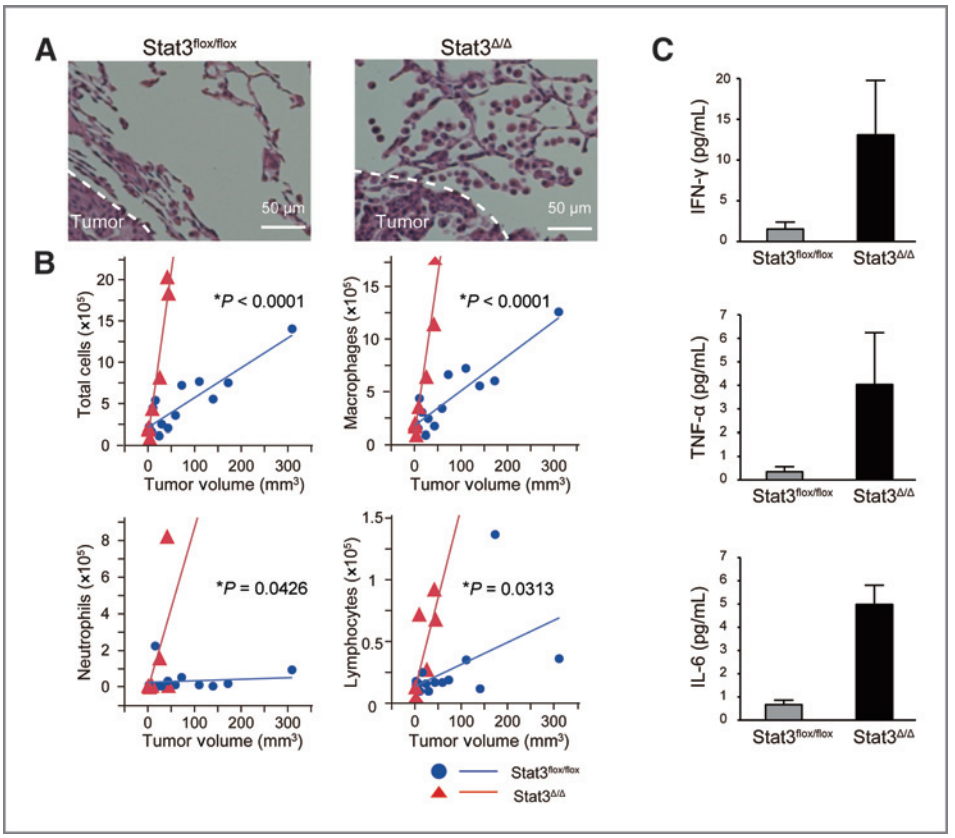

Figure 3. Tumor-associated inflammation was increased in Stat3$^{\Delta/\Delta}$. A, representative H&E-stained sections of the peripheral area of lung tumors, showing significantly more inflammatory cell accumulation in Stat3$^{\Delta/\Delta}$ mice compared with Stat3$^{flox/flox}$ mice. B, the total number of cells, macrophages, neutrophils, and lymphocytes in BAL were plotted versus the total lung tumor volume. $N = 14$ for Stat3$^{flox/flox}$ group and $N = 8$ for Stat3$^{\Delta/\Delta}$ group. The P values for the interaction by ANOVA are shown in each graph. C, the concentrations of IFN-γ, TNF-α, and IL-6 were measured and normalized to the total lung tumor volume. $N = 3$ per group.

in Fig. 5D, cellular migration was considerably promoted in the presence of culture supernatants from Stat3 siRNA–transfected NSCLC cells. These findings support the hypothesis that inhibition of Stat3 signaling in tumor cells promotes the production of chemotactic factors that enhance antitumor immunity.

Stat3 increased MHC class I expression in tumor cells and inactivated NK cells

NK cells attack malignant cells with impaired MHC class I expression (2). To confirm the results of the microarray analysis, which showed that a Stat3 deletion results in the downregulation of MHC class I in tumor cells, we examined the expression of MHC class I in tumor-bearing lung tissues from Stat3$^{\Delta/\Delta}$ mice. Western blot analysis using an antibody against mouse MHC class I revealed that MHC class I expression was decreased in tumor-bearing lung tissues from Stat3$^{\Delta/\Delta}$ mice compared with Stat3$^{flox/flox}$ mice (Fig. 6A). siRNA-mediated knockdown of Stat3 also decreased MHC class I expression in human lung cancer cell lines (Fig. 6B). We finally tested whether Stat3 activation affects NK cell cytotoxic activities against tumor cells using ^{51}Cr-release assays with NSCLC cells (H3255 and H441) that were transfected with Stat3 siRNA. Stat3 knockdown increased the susceptibility of NSCLC cells to NK cell–mediated cytotoxicity (Fig. 6C). These data indicated that Stat3 deletion in tumor cells downregulates the expression of the MHC class I to stimulate NK cell–mediated antitumor immunity.

Discussion

In this study, we investigated the role of Stat3 in carcinogen-induced lung tumorigenesis. Although Stat3 has been implicated in tumor growth, survival, and angiogenesis, we unexpectedly found that proliferation, apoptosis, and angiogenesis were not altered in Stat3$^{\Delta/\Delta}$ lung tumors. Instead, we found that tumorigenesis was significantly reduced in Stat3$^{\Delta/\Delta}$ mice, whereas tumor-associated inflammation was increased. We further carried out genome-wide mRNA profiling and found that Stat3 knockdown increased the expression of proinflammatory chemokines and decreased the expression of MHC class I. Thus, we provide evidence that Stat3 negatively regulates antitumor immunity during lung tumorigenesis.

Inhibitory roles of Stat3 in antitumor immunity during carcinogen-induced tumorigenesis

The role of Stat3 in inflammation-associated tumorigenesis has been extensively investigated in several organs, including the colon (15, 16), stomach (17), and pancreas (18, 19). These studies indicated that Stat3 activation increases cancer-associated inflammation to promote proliferation and inhibit tumor cell apoptosis. In addition, it was reported that overexpressing a constitutively active Stat3 in airway epithelial cells in the lung promoted lung inflammation and tumor formation (31). However, the roles of Stat3 in antitumor immunity during lung tumorigenesis have not been determined. In this study, we

Published OnlineFirst June 1, 2012; DOI: 10.1158/0008-5472.CAN-11-4062

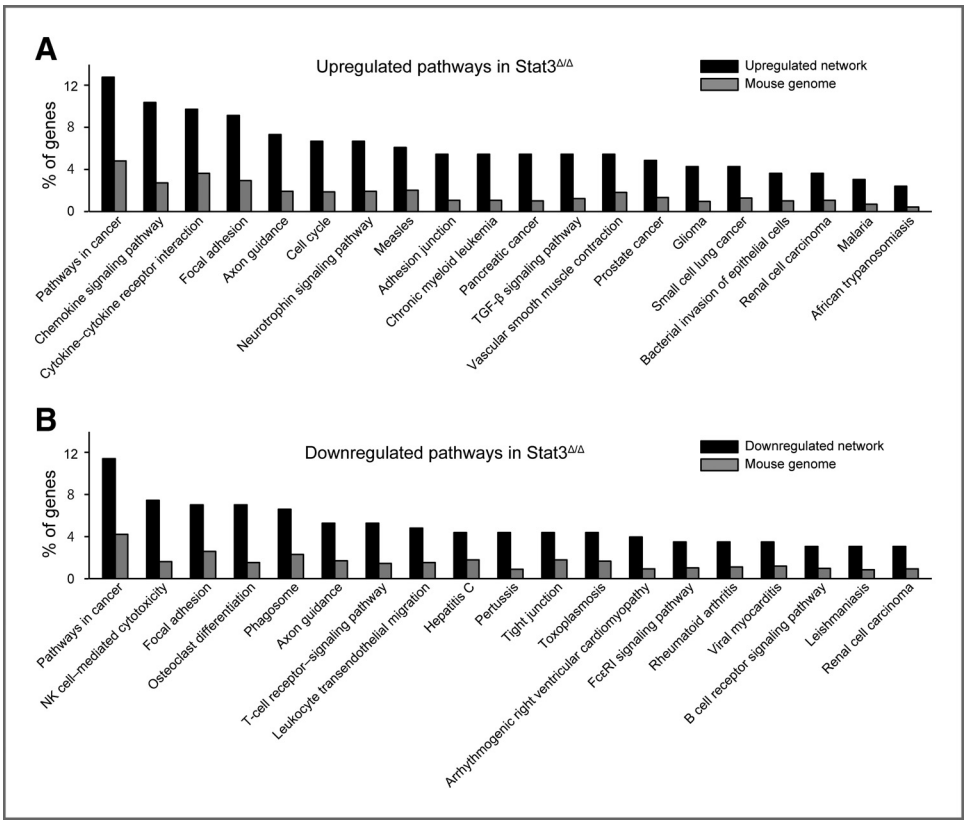

Figure 4. Microarray data revealed significant pathways associated with increased tumor-associated inflammation in Stat3$^{\Delta/\Delta}$ mice. KEGG pathway associations enriched in upregulated (A) and downregulated (B) PPI networks. The pathway labels are mapped on the x-axis, whereas the y-axis represents the percentage of genes that mapped to a given KEGG pathway within the network and the mouse genome.

examined a carcinogen-induced lung tumorigenesis model and found that Stat3 plays a novel role in negatively regulating antitumor immunity. Indeed, NSCLC is not strongly associated with inflammation compared with cancers in other organs (20–22). In our studies, tumor-associated inflammation increased in Stat3$^{\Delta/\Delta}$ mice, which exhibited reduced tumorigenesis. According to the increased inflammation in Stat3$^{\Delta/\Delta}$ lungs, antitumor inflammatory mediators such as TNF-α and IFN-γ were elevated in the lungs of Stat3$^{\Delta/\Delta}$ mice compared with Stat3$^{flox/flox}$ mice, although we carefully evaluated their local concentrations. By contrast, we did not observe any differences in proliferation, apoptosis, or angiogenesis between Stat3$^{\Delta/\Delta}$ and Stat3$^{flox/flox}$ tumors. Although previous studies indicate that Stat3 has mitotic and antiapoptotic roles in cancer cell lines (10–13), we did not observe these Stat3-related effects in our model. Stat3 might inhibit antitumor immunity in the early phase of tumorigenesis to alter the tumor microenvironment and promote proliferation or survival in the late phase of tumorigenesis. Taken together, our findings indicate that the inflammation observed in the lungs of Stat3$^{\Delta/\Delta}$ mice had anticancer effects. Further studies are required to determine how Stat3 differentially regulates antitumor immunity in different organs.

Negative regulation of chemokine production by Stat3

Here, we showed that Stat3 negatively regulates chemokine genes, including CCL5 and CXCL10, which play important roles in cancer-associated inflammation by attracting various subpopulations of immune effector cells (32, 33). Consistent with this finding, Wang and colleagues reported that constitutively active Stat3 inhibits the production of multiple proinflammatory cytokines and chemokines in mouse cancer cell lines (34).

Mice with a selective disruption of Stat3 in keratinocytes were reported to have defective wound healing associated with increased inflammatory infiltrates at the wound sites (35). Thus, Stat3-mediated inhibition of proinflammatory factors affects not only the tumor microenvironment but also the site of physiologic wound healing.

With regard to the gene regulation by Stat3, Xu Y and colleagues previously reported the effects of a pulmonary epithelial cell–specific deletion of Stat3 using genome-wide mRNA expression profiling, in which they found that chemotaxis-related genes were significantly induced by a Stat3 deletion, and these authors also reported that *STAT* was the most significantly enriched cis-element in the promoter region of differentially expressed genes, suggesting that Stat3 directly controls the expression of these genes (36).

Decreased MHC class I expression in tumor cells augments antitumor inflammation

We provided evidence that inhibition of Stat3 signals in tumor cells decreased the expression of MHC class I in tumor cells, resulting in enhanced NK cell cytotoxic activities. This raises the question of whether the decreased MHC class I expression in tumor cells affects adaptive antitumor immunity

Published OnlineFirst June 1, 2012; DOI: 10.1158/0008-5472.CAN-11-4062

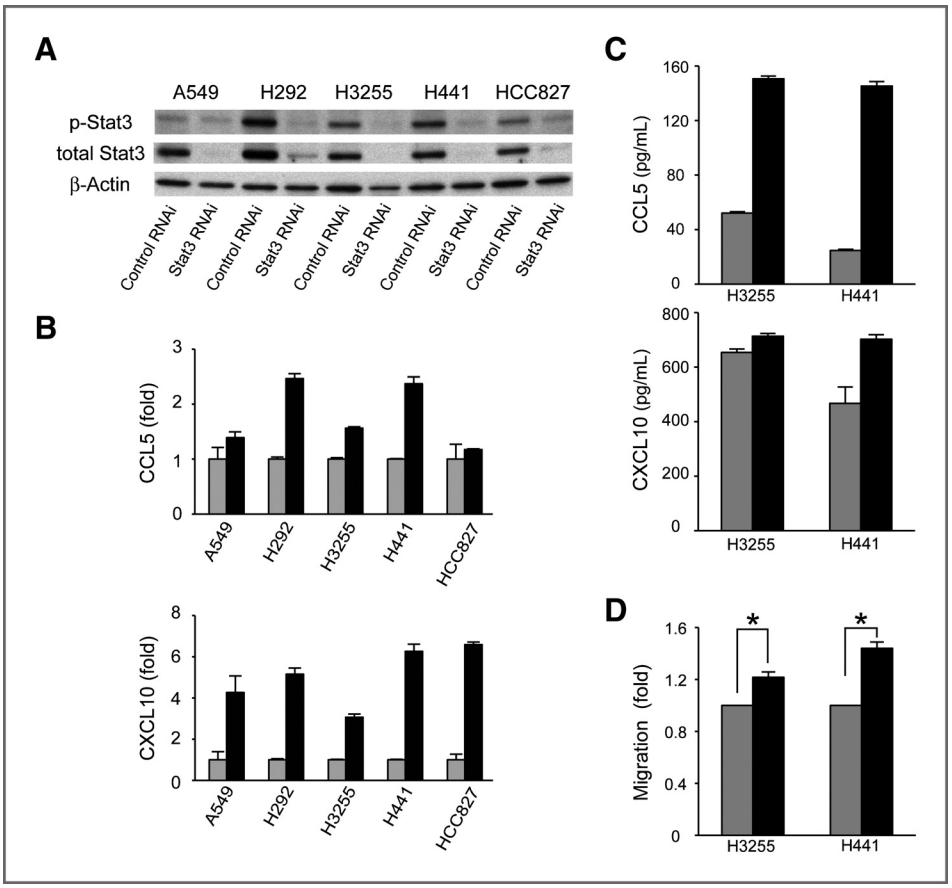

Figure 5. Stat3 knockdown increased the ability of lung tumors to attract leukocytes. A, immunoblot analysis of phospho-Stat3 and total Stat3 in lysates prepared from various NSCLC cell lines that were transfected with control or Stat3 siRNA. B, relative mRNA expression levels of chemokines in various NSCLC cell lines that were transfected with control or Stat3 siRNA. Results were standardized to the GAPDH mRNA levels and normalized to control siRNA-transfected cells. Data are representative of 3 independent experiments. C, protein concentrations of CCL5 and CXCL10 in the culture supernatant of NSCLC cell lines (H3255 and H441) that were transfected with control or Stat3 siRNA. Data are representative of 3 independent experiments. D, an *in vitro* migration assays revealed that the culture supernatant of NSCLC cell lines transfected with Stat3 siRNA contained more chemoattractants for monocytes (THP-1). Results were normalized to the control siRNA and are presented as the means ± SE of 3 experiments. B to D, gray and black bars represent control siRNA and Stat3 siRNA, respectively. *, $P < 0.05$.

mediated by $CD8^+$ T cells. Indeed, Schreiber and colleagues reported that, although NK cells are important in the early elimination of tumors, the "dormant" tumor state is controlled by adaptive immunity mediated by $CD8^+$ T cells (37). However, it has been reported that MHC class I–low tumor cells still evoke antitumor $CD8^+$ T-cell responses because NK cells, activated by MHC class I–low tumor cells, produce IFN-γ that stimulates $CD8^+$ T cells (38, 39). Thus, enhanced NK cell responses, together with increased chemokine production by tumor cells, may be primarily responsible for antitumor inflammation during urethane-induced tumors. It is also noteworthy that the efficacy of the antitumor cytotoxic activities of cytotoxic $CD8^+$ T cells (CTL) depends not only on the presentation of tumor antigens by the malignant cells but also on their susceptibility to $CD8^+$ T-cell–induced lysis. The hypoxic tumor microenvironment confers resistance to this CTL-mediated cytotoxic activity. Interestingly, it was recently reported that Stat3 and hypoxia-inducible factor (HIF)-1α are functionally linked to the alteration of NSCLC susceptibility to CTL-mediated killing under hypoxic conditions (40). In this context, Stat3 activation in tumor cells may affect tumor cell sensitivity to either NK cell– or $CD8^+$ T-cell–mediated cell killing.

With regard to the regulation of MHC class I expression by Stat3, there are several possibilities, which affect MHC class I expression during tumorigenesis, such as inflammatory cytokines, oncogenic transcriptional factors, and tumor-associated missing self-phenotypes. Further studies are necessary to clarify the mechanism of how Stat3 regulates the expression of MHC class I molecule.

Involvement of Stat3 in tumorigenesis and its clinical implication

Adenocarcinoma is the most common histologic type of lung cancer, accounting for almost half of all lung cancers. The relevant molecular events frequently observed in lung adenocarcinoma are *KRAS* mutations, epidermal growth factor receptor mutations, and echinoderm microtubule–associated protein-like 4-anaplastic lymphoma kinase translocations (41). Stat3 is activated and responsible for the oncogenic phenotypes of adenocarcinoma caused by such molecular mutations or alterations (18, 19, 42, 43). Thus, it is possible that Stat3 inhibition not only promotes antitumor immunity but also impairs oncogenic signals in adenocarcinoma. Indeed, several reports suggest that Stat3 activation is relevant to the progression of human NSCLC (44, 45); however, it may be difficult to determine the involvement of Stat3 activation in the *in vivo* tumorigenesis of NSCLC. We therefore think that our *in vivo* tumorigenesis model provides a clue to understand the involvement of Stat3 activation in NSCLC tumorigenesis. Collectively, our findings not only indicate a novel role for Stat3 in lung tumorigenesis but also provide a potential therapeutic target for lung cancers.

Published OnlineFirst June 1, 2012; DOI: 10.1158/0008-5472.CAN-11-4062

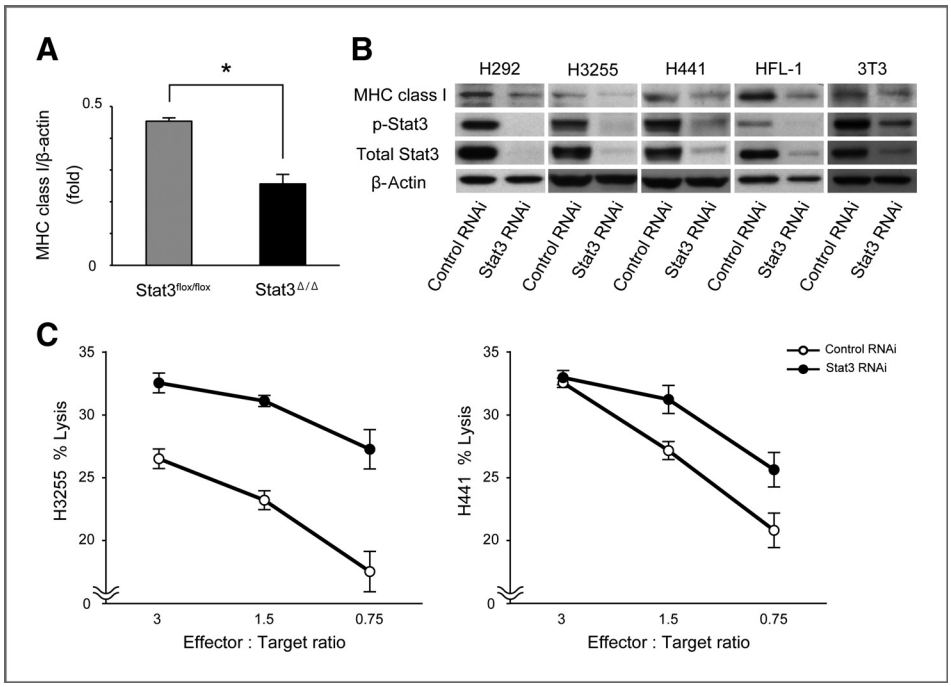

Figure 6. Stat3 knockdown decreased MHC class I expression on lung tumor cells, resulting in the activation of NK cell–mediated cytotoxicity. A, immunoblot analysis of MHC class I in lung homogenates from $Stat3^{flox/flox}$ mice and $Stat3^{\Delta/\Delta}$ mice. $N = 3$ per group. *, $P < 0.05$. B, immunoblot analysis of MHC class I in lysates prepared from a series of NSCLC cell lines that were transfected with control or Stat3 siRNA. C, a cytotoxic assay revealed that Stat3 knockdown increased the susceptibility of an NSCLC cell line (H3255 and H441) to NK cell–mediated cytotoxicity. Results are representative of 3 experiments.

Disclosure of Potential Conflicts of Interest

No potential conflicts of interest were disclosed.

Authors' Contributions

Conception and design: S. Ihara, H. Kida, M. Yoshida, A. Kumanogoh
Development of methodology: S. Ihara, L.P. Tripathi, Y.-A. Chen, K. Mizuguchi
Acquisition of data (provided animals, acquired and managed patients, provided facilities, etc.): S. Ihara, H. Kida, L.P. Tripathi, Y.-A. Chen, T. Kimura, Y. Kashiwa, R. Inoue, K. Hasegawa, T. Minami, M. Suzuki, S. Kohmo, I. Nagatomo, T. Kijima, I. Tachibana
Analysis and interpretation of data (e.g., statistical analysis, biostatistics, computational analysis): S. Ihara, H. Kida, L.P. Tripathi, Y.-A. Chen, M. Yoshida, Y. Kashiwa, H. Hirata, R. Inoue, K. Hasegawa, R. Takahashi, T. Minami, M. Suzuki, S. Kohmo, I. Nagatomo, Y. Takeda, T. Kijima, K. Mizuguchi, I. Tachibana
Writing, review, and/or revision of the manuscript: S. Ihara, H. Kida, L.P. Tripathi, Y.-A. Chen, K. Tsujino, K. Mizuguchi, A. Kumanogoh
Administrative, technical, or material support (i.e., reporting or organizing data, constructing databases): S. Ihara, H. Arase, T. Kimura, R. Fukamizu, K. Tsujino
Study supervision: H. Kida, H. Arase, M. Yoshida, S. Goya, K. Inoue, A. Kumanogoh

Acknowledgments

The authors thank Jeffrey A. Whitsett (Cincinnati, OH) for the kind gift of $Stat3^{\Delta/\Delta}$.

Grant Support

The work was support by KAKENHI (20890116), and a grant from the Osaka Foundation for Promotion of Clinical Immunology to H. Kida, Industrial Technology Research Grant Program in 2007 to K. Mizuguchi from the New Energy and Industrial Technology Development Organization (NEDO) of Japan, a grant from Program for Promotion of Fundamental Studies in Health Science of the National Institute of Biomedical Innovation to I. Tachibana, and Funding Program for Next Generation World-Leading Researchers (NEXT Program), and Special Coordination Funds for Promoting Science and Technology to A. Kumanogoh.

The costs of publication of this article were defrayed in part by the payment of page charges. This article must therefore be hereby marked *advertisement* in accordance with 18 U.S.C. Section 1734 solely to indicate this fact.

Received December 19, 2011; revised March 15, 2012; accepted March 27, 2012; published OnlineFirst June 1, 2012.

References

1. Mantovani A, Allavena P, Sica A, Balkwill F. Cancer-related inflammation. Nature 2008;454:436–44.
2. Dunn GP, Bruce AT, Ikeda H, Old LJ, Schreiber RD. Cancer immunoediting: from immunosurveillance to tumor escape. Nat Immunol 2002;3:991–8.
3. Pagès F, Galon J, Dieu-Nosjean MC, Tartour E, Sautès-Fridman C, Fridman WH. Immune infiltration in human tumors: a prognostic factor that should not be ignored. Oncogene 2010;29:1093–102.
4. Nelson BH. The impact of T-cell immunity on ovarian cancer outcomes. Immunol Rev 2008;222:101–16.
5. Teng MWL, Swann JB, Koebel CM, Schreiber RD, Smyth MJ. Immune-mediated dormancy: an equilibrium with cancer. J Leukoc Biol 2008;84:988–93.
6. Kim R, Emi M, Tanabe K. Cancer immunoediting from immune surveillance to immune escape. Immunology 2007;121:1–14.
7. Ostrand-Rosenberg S, Sinha P. Myeloid-derived suppressor cells: Linking inflammation and cancer. J Immunol 2009;182:4499–506.
8. Takeda K, Noguchi K, Shi W, Tanaka T, Matsumoto M, Yoshida N, et al. Targeted disruption of the mouse Stat3 gene leads to early embryonic lethality. Proc Natl Acad Sci U S A 1997;94:3801–4.
9. Akira S. Role of Stat3 defined by tissue-specific gene targeting. Oncogene 2000;19:2607–11.
10. Catlett-Falcone R, Landowski TH, Oshiro MM, Turkson J, Levitzki A, Savino R, et al. Constitutive activation of Stat3 signaling confers resistance to apoptosis in human U266 myeloma cells. Immunity 1999;10:105–15.
11. Epling-Burnette PK, Liu JH, Catlett-Falcone R, Turkson J, Oshiro M, Kothapalli R, et al. Inhibition of STAT3 signaling leads to apoptosis of leukemic large granular lymphocytes and decreased Mcl-1 expression. J Clin Invest 2001;107:351–62.

Published OnlineFirst June 1, 2012; DOI: 10.1158/0008-5472.CAN-11-4062

12. Sinibaldi D, Wharton W, Turkson J, Bowman T, Pledger WJ, Jove R. Induction of $p21^{WAF1/CIP1}$ and cyclin D1 expression by the Src oncoprotein in mouse fibroblasts: role of activated STAT3 signaling. Oncogene 2000;19:5419–27.
13. Bowman T, Broome MA, Sinibaldi D, Wharton W, Pledger WJ, Sedivy JM, et al. Stat3-mediated Myc expression is required for Src transformation and PDGF-induced mitogenesis. Proc Natl Acad Sci U S A 2001;98:7319–24.
14. Yu H, Kortylewski M, Pardoll D. Crosstalk between cancer and immune cells: role of STAT3 in the tumour microenvironment. Nat Rev Immunol 2007;7:41–51.
15. Bollrath J, Phesse TJ, von Burstin VA, Putoczki T, Bennecke M, Bateman T, et al. Gp130-mediated Stat3 activation in enterocytes regulates cell survival and cell-cycle progression during colitis-associated tumorigenesis. Cancer Cell 2009;15:91–102.
16. Grivennikov S, Karin E, Terzic J, Mucida D, Yu GY, Vallabhapurapu S, et al. IL-6 and Stat3 are required for survival of intestinal epithelial cells and development of colitis-associated cancer. Cancer Cell 2009;15:103–13.
17. Ernst M, Najdovska M, Grail D, Lundgren-May T, Buchert M, Tye H, et al. STAT3 and STAT1 mediate IL-11-dependent and inflammation-associated gastric tumorigenesis in gp130 receptor mutant mice. J Clin Invest 2008;118:1727–38.
18. Fukuda A, Wang SC, Morris JP, Folias AE, Liou A, Kim GE, et al. Stat3 and MMP7 contribute to pancreatic ductal adenocarcinoma initiation and progression. Cancer Cell 2011;19:441–55.
19. Lesina M, Kurkowski MU, Ludes K, Rose-John S, Treiber M, Klöppel G, et al. Stat3/Socs3 activation by IL-6 transsignaling promotes progression of pancreatic intraepithelial neoplasia and development of pancreatic cancer. Cancer Cell 2011;19,456–69.
20. Coussens LM, Werb Z. Inflammation and cancer. Nature 2002;420:860–7.
21. Kisley LR, Barrett BS, Dwyer-Nield LD, Bauer AK, Thompson DC, Malkinson AM. Celecoxib reduces pulmonary inflammation but not lung tumorigenesis in mice. Carcinogenesis 2002;23:1653–60.
22. Doris K, Karabela1 SP, Kairi CA, Simoes DCM, Roussos C, Zakynthinos SG, et al. Allergic inflammation does not impact chemical-induced carcinogenesis in the lungs of mice. Respir Res 2010;11:118–27.
23. Perl AK, Wert SE, Nagy A, Lobe CG, Whitsett JA: Early restriction of peripheral and proximal cell lineages during formation of the lung. Proc Natl Acad Sci U S A 2002;99:10482–7.
24. Hokuto I, Ikegami M, Yoshida M, Takeda K, Akira S, Perl AK, et al. Stat-3 is required for pulmonary homeostasis during hyperoxia. J Clin Invest 2004;113:28–37.
25. Stark C, Breitkreutz BJ, Reguly T, Boucher L, Breitkreutz A, Tyers M. BioGRID: a general repository for interaction datasets. Nucleic Acids Res 2006;34:D535–9.
26. Turner B, Razick S, Turinsky AL, Vlasblom J, Crowdy EK, Cho E, et al. iRefWeb: interactive analysis of consolidated protein interaction data and their supporting evidence. Database (Oxford) 2010;2010:baq023.
27. Chen YA, Tripathi LP, Mizuguchi K. TargetMine, an integrated data warehouse for candidate gene prioritisation and target discovery. PLoS One 2011;6:e17844.
28. Aoki-Kinoshita K F, Kanehisa M. Gene annotation and pathway mapping in KEGG. Methods Mol Biol 2007;396:71–91.
29. Benjamini Y, Hochberg Y. Controlling the false discovery rate—A practical and powerful approach to multiple testing. J R Statist Soc 1995;B57:289–300.
30. Whiteside TL. Measurement of cytotoxic activity of NK/LAK cells. Curr Protoc Immunol 2001;7:17.18.
31. Li Y, Du H, Qin Y, Roberts J, Cummings OW, Yan C. Activation of the signal transducers and activators of the transcription 3 pathway in alveolar epithelial cells induces inflammation and adenocarcinomas in mouse lung. Cancer Res 2007;67:8494–503.
32. Mulé JJ, Custer M, Averbook B, Yang JC, Weber JS, Goeddel DV, et al. RANTES secretion by gene-modified tumor cells results in loss of tumorigenicity *in vivo:* role of immune cell subpopulations. Hum Gene Ther 1996;7:1545–53.
33. Fujita M, Zhu X, Ueda R, Sasaki K, Kohanbash G, Kastenhuber ER, et al. Effective immunotherapy against murine gliomas using type 1 polarizing dendritic cells–Significant roles of CXCL10. Cancer Res 2009;69:1587–95.
34. Wang T, Niu G, Kortylewski M, Burdelya L, Shain K, Zhang S, et al. Regulation of the innate and adaptive immune responses by Stat-3 signaling in tumor cells. Nat Med 2004;10:48–54.
35. Sano S, Itami S, Takeda K, Tarutani M, Yamaguchi Y, Miura H, et al. Keratinocyte-specific ablation of Stat3 exhibits impaired skin remodeling, but does not affect skin morphogenesis. EMBO J 1999;18:4657–68.
36. Xu Y, Ikegami M, Wang Y, Matsuzaki Y, Whitsett JA. Gene expression and biological processes influenced by deletion of *Stat3* in pulmonary type II epithelial cells. BMC Genomics 2007;8:455.
37. Koebel CM, Vermi W, Swann JB, Zerafa N, Rodig SJ, Old LJ, et al. Adaptive immunity maintains occult cancer in an equilibrium state. Nature 2007;450:903–7.
38. Mocika Rt, Braumüller H, Gumy A, Egeter O, Ziegler H, Reusch U, et al. Natural killer cells activated by MHC class I^{Low} targets prime dendritic cells to induce protective CD8 T cell responses. Immunity 2003;19:561–9.
39. Adam C, King S, Allgeier T, Braumüller H, Lüking C, Mysliwietz J, et al. DC-NK cell cross talk as a novel CD4+ T-cell–independent pathway for antitumor CTL induction. Blood 2005;106:338–44.
40. Noman MZ, Buart S, Pelt JV, Richon C, Hasmim M, Leleu N, et al. The cooperative induction of hypoxia-inducible factor-1α and STAT3 during hypoxia induced an impairment of tumor susceptibility to CTL-mediated cell lysis. J Immunol 2009;182:3510–21.
41. Travis WD, Brambilla E, Noguchi M, Nicholson AG, Geisinger KR, Yatabe Y, et al. International Association for the Study of Lung Cancer/American Thoracic Society/European Respiratory Society International Multidisciplinary Classification of Lung Adenocarcinoma. J Thorac Oncol 2011;6:244–85
42. Gao SP, Mark KG, Leslie K, Pao W, Motoi N, Gerald WL, et al. Mutations in the EGFR kinase domain mediate STAT3 activation via IL-6 production in human lung adenocarcinoma. J Clin Invest 2007;117:3846–56.
43. Takezawa K, Okamoto I, Nishio K, Janne PA, Nakagawa K. Role of ERK-BIM and STAT3-Survivin signaling pathways in ALK inhibitor–induced apoptosis in EML4-ALK–positive lung cancer. Clin Cancer Res 2011;17:2140–8.
44. Haura EB, Zheng Z, Song L, Cantor A, Bepler G. Activated epidermal growth factor receptor-Stat3 signaling promotes tumor survival *in vivo* in non-small cell lung cancer. Clin Cancer Res 2005;11:8288–94.
45. Yeh HH, Lai WW, Chen HHW, Liu HS, Su WC. Autocrine IL-6-induced Stat3 activation contributes to the pathogenesis of lung adenocarcinoma and malignant pleural effusion. Oncogene 2006;25:300–4309.

Published OnlineFirst June 1, 2012; DOI: 10.1158/0008-5472.CAN-11-4062

Cancer Research
The Journal of Cancer Research (1916–1930) | The American Journal of Cancer (1931–1940)

AACR American Association for Cancer Research

Inhibitory Roles of Signal Transducer and Activator of Transcription 3 in Antitumor Immunity during Carcinogen-Induced Lung Tumorigenesis

Shoichi Ihara, Hiroshi Kida, Hisashi Arase, et al.

Cancer Res Published OnlineFirst June 1, 2012.